Characterization of the Internal and External Acidity of H-MCM-22 Zeolites

P. Ayrault,[†] J. Datka,[‡] S. Laforge,[†] D. Martin,[†] and M. Guisnet*[,†]

Laboratoire de Catalyze en Chimie Organique, Faculté des Sciences, Université de Poitiers, UMR CNRS 6503, 40, avenue du Recteur Pineau, 86022 Poitiers Cedex, France, and Department of Chemistry, Jagiellonian University, Ingardena 3, 30-060 Cracow, Poland

Received: April 22, 2004; In Final Form: July 7, 2004

Adsorption of pyridine and of bulkier bases, 2,6- and 2,4-dimethylquinoline (DMQ), was carried out over five H-MCM-22 (MWW) samples differing by their Si/Al ratio (10, 17, 29, 50, 53) and their external surface area (49, 114, 102, 55, 33 $m^2 \cdot g^{-1}$). The comparison of the IR spectra of 2,6- and 2,4-DMQ pure or adsorbed on silica, alumina and large pore zeolites (H−BEA) shows that physisorbed and hydrogen bonded species can be eliminated by evacuation above 473 K. Because of steric hindrance, DMQ molecules do not interact with Lewis sites and hence can only be chemisorbed as dimethylquinolinium ions (DMQ^+). Extinction coefficients were estimated for characteristic bands at 1547 and 1649 cm^{-1} (2,6-DMQ^+), at 1647 cm^{-1} (2,4-DMQ^+) and at 3620 cm^{-1} (bridging hydroxyl groups). For adsorption temperatures of 473−573 K, 2,6-DMQ molecules were protonated on most of the protonic sites of the H-MCM-22 samples. The bulkier 2,4-DMQ molecules can be protonated only on part of the inner sites (most likely those located near the surface of crystallite edges) and on the protonic sites of the external pockets. The concentration of the latter sites can be estimated from the difference between the concentrations of 2,4-DMQ^+ ions and of the inner bridging hydroxyl groups (IR band at 3620 cm^{-1}) which interact with 2,4-DMQ molecules. This concentration was found to be close to the one of external pocket sites active in *m*-xylene transformation at 623 K. It is also proportional to the external surface area. All that indicates that 2,4-DMQ chemisorption followed by IR spectroscopy is a suitable method for characterizing the outer acidity of H-MCM-22 zeolites.

Introduction

MCM-22 zeolite[1] has the particularity to possess two independent pore systems.[2] One pore system is constituted by two-dimensional sinusoidal intersecting channels with an elliptical 10 MR ring cross section (4.1 × 5.1 Å). The other system possesses large cylindrical supercages with a diameter defined by a 12 MR (7.1 Å) and a height of 18.2 Å; these supercages are accessible through 10 MR apertures (4.0 × 5.5 Å). In addition, half supercages form large pockets (7.1 Å o.d. × 9.0 Å height) on the outer [001] crystal surfaces.[3] MCM-22 zeolites crystallize under the form of fine plates,[4,5] which gives them a relatively large outer surface area. The majority of this outer surface is on the [001] crystal faces with the large pockets, the other part, which contains the 10 MR apertures of the inner pores, corresponding to the thin crystal edges.[3]

Acidic bridged OH groups (SiOHAl) may be located not only in the inner pores but also in the external pockets, which explains that in many hydrocarbon reactions, the product selectivity of H-MCM-22 catalysts is between those of large and medium pore size zeolites.[6−14] In certain reactions, the protonic acid sites located in the external pockets could be the only active sites.[15,16] This was shown for benzene alkylation with ethylene:[17,18] poisoning with 2,4,6-trimethylpyridine (γ-collidine) causes a quasicomplete deactivation of the MCM-22 catalyst, this deactivation being only due to the selective poisoning of the outer pockets sites. Indeed, collidine molecules are too bulky (cross section of 6.2 × 5.6 Å) to enter the intracrystalline pore systems. Furthermore, chemisorbed collidine was shown to have no effect on 3-methylpentane and ethylbenzene sorption rates and hence does not cause any limitation in the access to the inner acid sites.[18] Last, no physisorbed collidine molecules were present under the operating conditions.[18]

Selective poisoning with collidine could also be used to estimate the catalytic role of the external pockets in reactions occurring both on the inner and the outer acidic sites of MCM-22 zeolites. Unfortunately, collidine desorbs from the outer protonic sites from 473 K,[18] which limits its use to reactions carried out at low temperatures. It is why in *m*-xylene transformation at 623 K, we have used other bulky basic poisons, i.e., 2,6- and 2,4-dimethylquinoline (2,6- and 2,4-DMQ).[19] 2,6-DMQ was shown to poison all the MCM-22 acidic sites (external and inner). 2,4-DMQ which is bulkier selectively poisons the external active sites. Indeed, there is a good agreement between the estimated product distribution and the one expected from the shape and size of the external pockets: mainly isomerization with a *p*- to *o*-xylene ratio of 1.1 i.e., close to the one obtained over large pore zeolites such as FAU (non shape selective process). With the method employed for MCM-22 poisoning with 2,4-DMQ, it was also possible to estimate the number of active external acid sites. This number was found equal to approximately 9% of all the protonic sites of the MCM-22 sample (able to retain pyridine adsorbed at 423 K). This percentage is close to the one of external acid sites estimated by other authors through various methods: adsorption of 2,6-diterbutylpyridine followed by IR spectroscopy (6%),[20] and thermodesorption of collidine (12%),[18] PPh_3 adsorption followed by ^{31}P MAS NMR (6%)[21] and ^{27}Al 2D-5Q MAS NMR (10%).[22]

* To whom correspondence should be addressed. Telephone: + 33-(0)5-49-45-39-05. Fax: + 33-(0)5-49-45-37-79. E-mail: michel.guisnet@univ-poitiers.fr.

[†] Université de Poitiers.

[‡] Jagiellonian University.

10.1021/jp048242z CCC: $27.50
Published on Web 08/18/2004

TABLE 1: Chemical Composition and Porosity of the H-MCM-22 Samples[a]

sample	Si/Al	V_{total} ($cm^3.g^{-1}$)	V_{micro} ($cm^3.g^{-1}$)	V_{ultra} ($cm^3.g^{-1}$)	V_{super} ($cm^3.g^{-1}$)	V_{meso} ($cm^3.g^{-1}$)	S_{BET} ($m^2.g^{-1}$)	S_{ext} ($m^2.g^{-1}$)
MCM-22 (1)	10	0.413	0.209	0.197	0.012	0.204	512	49
MCM-22 (2)	17	0.520	0.220	0.180	0.040	0.300	551	114
MCM-22 (3)	29	0.620	0.216	0.180	0.036	0.404	544	102
MCM-22 (4)	50	0.364	0.198	0.187	0.011	0.166	478	55
MCM-22 (5)	53	0.309	0.195	0.183	0.012	0.114	484	33

[a] Total Si/Al ratio, determined by chemical analysis. V_{total}: total pore volume at $P/P_0 = 0.97$. V_{micro}: micropore volume. V_{super}: volume of the micropores with a diameter of 0.8 to 2.0 nm (supermicropores). V_{ultra}: volume of the micropores with a diameter smaller than 0.8 nm (ultramicropores). S_{BET}: BET surface area. S_{ext}: external surface area.

Preliminary experiments of 2,4-DMQ adsorption followed by IR spectroscopy suggested that a good estimation of the concentration of the outer acidic sites could be obtained with this method.[19] It is the aim of this paper to confirm the validity of this method. For that, 2,4-DMQ adsorption was studied on five H-MCM-22 samples with different external surface areas (from 33 to 114 $m^2 \cdot g^{-1}$) and hence with different percentages of external acid sites. As a comparison, 2,6-DMQ adsorption was also carried out on the same samples. The concentrations of the external acid sites obtained through 2,4-DMQ adsorption will be compared to those deduced from poisoning experiments of *m*-xylene transformation.

Experimental Section

1. Preparation of the Materials. The MCM-22 precursors (MCM-22 (P)) were prepared in the Instituto de Tecnologia Quimica of Valencia (Spain) according to the method reported in the literature[1,4] and then calcined under air at 623 K for 2 h and then at 853 K for 3 h in order to obtain the final MCM-22 zeolite structure.

The protonic forms of the MCM-22 were obtained by two successive cationic exchanges with a 2 M NH_4Cl solution at 353 K for 1 h and then calcination at 623 K for 2 h and at 773 K for 3 h.

2. Characterization of the Samples. 2.1. Structure and Porosity. The structural type and crystallinity of the different samples were verified through powder X-ray diffraction (XRD) on a Philips PW1800 diffractometer with Cu Kα radiation ($\lambda = 1.5406$ Å).

Nitrogen adsorption measurements were carried out at 77 K on a Micromeritics Tristar apparatus. Before adsorption, the samples were pretreated at 623 K under vacuum for 12 h. The specific surface area were determined by the Brunauer−Emmett−Teller (BET) method. The micropore and ultramicropore volumes were estimated by Dubinin−Raduskevitch and *t*-plot methods,[23] using the Harkins−Jura equation,[24] the supermicropore volume being the difference between the micropore and ultramicropore volumes. Finally, the external surface areas of the samples were estimated from the *t*-plots[25] and mesopore volumes were taken as the difference between the total and micropore volume (calculated from the Dubinin−Raduskevitch equation).

2.2. Acidic Properties. The acidic properties of the zeolite samples were characterized by adsorption of three basic molecules (pyridine and 2,6- and 2,4-dimethylquinoline) followed by IR spectroscopy, on a Nicolet 750 MAGNA-IRTM spectrometer. Prior to measurements, thin zeolite wafers (8−15 mg) were pretreated in situ at 723 °C for 12 h under air flow (60 $mL \cdot min^{-1}$) and then at 473 K for 1 h under vacuum (10^{-3} Pa).

Pyridine was introduced in excess (2−3 mbar) in the IR cell at 423 K. After outgassing at the same temperature (10^{-3} Pa, 1 h), to eliminate the physisorbed molecules, the concentrations of Brönsted and Lewis acid sites were calculated from the area of the bands at 1545 (pyridinium ions) and 1455 cm^{-1} (pyridine coordinated to Lewis sites), respectively, using the extinction coefficients previously determined.[26]

Contrary to pyridine, 2,6- and 2,4-dimethylquinoline are not enough volatile to be introduced in the gas phase. As a consequence, the following procedure was used. These compounds were solubilized in CH_2Cl_2 (20−40 μmol for 1 mL of solvent) and the solution was deposited homogeneously on the surface of the pretreated zeolite wafer. Then the solvent was evacuated in a vacuum (393 K), and IR spectra of adsorbed DMQ were recorded. The temperature was then increased, without evacuation (closed cell). After 20 min at 473 K (and then 573 K), the sample was evacuated in a vacuum and IR spectra were recorded.

3. *m*-Xylene Transformation. *m*-Xylene transformation was carried out under the following conditions: fixed bed glass reactor, 623 K, atmospheric pressure, $P_{N_2}/P_{mXyl} = 13$, contact time (taken as the reverse of the weight hourly space velocity) $\tau = 0.0087$ h. The reaction products were collected in a 10-position valve and analyzed in-line by a gas chromatograph (Varian 3800) equipped with a FID detector and a 60 m DB WAX (J&W Scientific) capillary column, with H_2 as the carrier gas.

Results and Discussion

1. Structure and Porosity of the H-MCM-22 Samples. Powder X-ray Diffraction patterns (not shown here) are similar to those reported in the literature.[4] All the H-MCM-22 samples were synthesized as pure phases, with a good crystallinity.

Table 1 shows that the micropore volumes of the H-MCM-22 samples are not very different and similar to those previously reported.[10,16,27−31] However, the supermicropore and mesopore volumes (most likely interparticular) as well as the external surface areas of the MCM-22 (2) and (3) samples are larger than those of the other samples, which can be related to a smaller size of their crystallites.

2. IR bands of Chemisorbed 2,6- and 2,4-DMQ Molecules. The IR spectra of 2,6- and 2,4-DMQ diluted in KBr (1 wt %) or adsorbed on a nonacidic support (SiO_2) were compared to those of these bases adsorbed on a typical Lewis acid solid (γAl_2O_3) and on two BEA samples, the first one (BEA-1) with equivalent concentrations of Brönsted and Lewis acid sites (315 and 340 $\mu mol \cdot g^{-1}$ respectively), the second one (BEA-2) with essentially Brönsted sites (84 $\mu mol \cdot g^{-1}$ against 8 $\mu mol \cdot g^{-1}$ of Lewis sites).[32] The aim was to determine the IR bands that are characteristic of 2,6- and 2,4-DMQ molecules chemisorbed on Brönsted (dimethylquinolinium ions, DMQ^+) and on Lewis sites.

2.1. IR Bands of Chemisorbed 2,6-DMQ Molecules. The spectra of 2,6-DMQ diluted in KBr, adsorbed on SiO_2 and on the BEA-1 zeolite, are presented in Figure 1, parts A and B. For spectra b and c, evacuation in a vacuum was carried out at

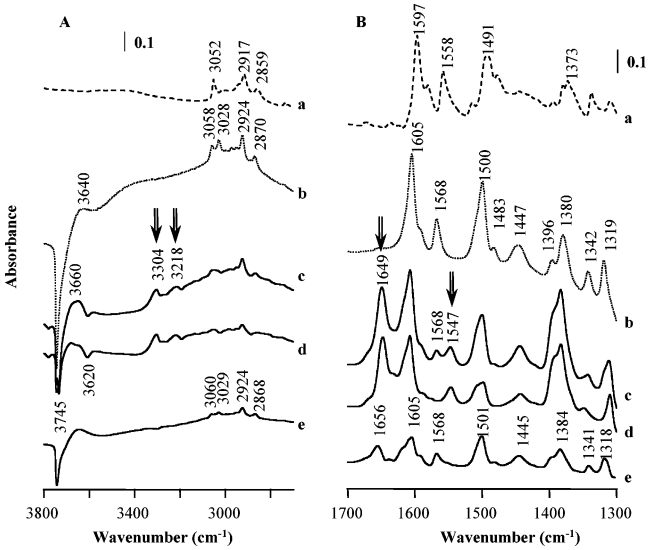

Figure 1. IR spectra of 2,6-dimethylquinoline (2,6-DMQ): (a) diluted in KBr; (b) adsorbed on SiO_2 at 393 K; (c, d) adsorbed on BEA-1 at 393 and 473 K, respectively (difference between the spectra after and before 2,6-DMQ adsorption); (e) difference spectrum (c − d).

393 K, for spectrum d it was at 473 K. After evacuation for 5 min at 393 K, the spectrum of 2,6-DMQ adsorbed on SiO_2 (b) is similar to the one of 2,6-DMQ in KBr (a), with however a shift of the bands to higher frequencies, probably due to interaction of 2,6-DMQ molecules with silanol groups. This interaction is demonstrated by a significant decrease of the silanol bands as well as by the appearance of a large new band at 3640 cm^{-1} (Figure 1A). Evacuation for 60 min at 393 K or for 20 min at 473 K leads to a complete desorption of 2,6-DMQ: complete disappearance of the 2,6-DMQ bands and of the 3640 cm^{-1} band and recovery of the silanol bands. All that is in favor of a weak interaction by hydrogen bond between 2,6-DMQ molecules and silanol groups. Adsorption of 2,6-DMQ on γ-alumina leads to a spectrum quite similar to spectrum b; moreover 2,6-DMQ is also completely removed by evacuation at 473 K. These observations indicate that only hydrogen bonded 2,6-DMQ molecules are present at 393 K on the alumina surface. The absence of interaction between 2,6-DMQ molecules and Lewis sites is, like in the case of lutidine,[33,34] most likely related to steric limitations in the access of the nitrogen atom to the Lewis sites, caused by the methyl group in position 2 (Scheme 1).

SCHEME 1

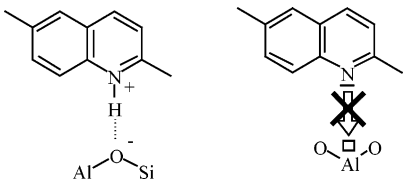

Spectrum c in Figure 1, parts A and B, shows that after evacuation for 5 min at 393 K of 2,6-DMQ adsorbed on BEA-1, there are several new bands, in particular at 1547, 1649 (ν_{C-C}), 3218, and 3304 cm^{-1} (ν_{N-H}) in addition to those corresponding to hydrogen bonded 2,6-DMQ molecules (spectrum b). 2,6-DMQ molecules interact with both silanol groups (large decrease of the silanol bands at 3745 cm^{-1} with appearance of a broad band at 3660 cm^{-1}) and with bridging hydroxyl groups (complete disappearance of the 3620 cm^{-1} band). Desorption at 473 K for 2 min (spectrum d) causes the complete disappearance of the band at 1568 cm^{-1}, a significant decrease of all the bands of hydrogen bonded 2,6-DMQ molecules and a partial recovery of the silanol bands.

Furthermore, the intensity of the new bands is practically unaffected (difference spectrum e = spectra c and d in Figure 1, parts A and B) and the bridging OH band is not recovered. It should be remarked that the band at 1656 cm^{-1} with can be clearly seen in spectrum e (Figure 1B) does not correspond to protonated 2,6-DMQ. Indeed, it is already present as a shoulder in spectra c and d.

From these observations it can be concluded that (i) all the hydrogen bonded 2,6-DMQ molecules can be desorbed by evacuation at 473 K (complete disappearance of the band at 1568 cm^{-1}), and (ii) spectrum d corresponds to the spectrum of 2,6-DMQ molecules chemisorbed on the BEA acid sites, the four new bands being characteristic of these chemisorbed molecules only. As 2,6-DMQ cannot chemisorb on the Lewis sites, spectrum d corresponds to 2,6-dimethylquinolinium ions (2,6-DMQ^+), resulting from the protonation of 2,6-DMQ molecules.

In agreement with the impossibility for 2,6-DMQ to strongly interact with Lewis sites, the bands which were observed with BEA-1 (spectrum d) can also be found with BEA-2, and in the same position (Figure 2, parts A and B, spectra a and b). Furthermore, the ratio between the intensities of the three characteristic bands found with the two zeolites (BEA-1/BEA-2 = 3.2−3.4) is not very different from the ratio of their protonic sites concentration (4.0).

2.2. IR Bands of Chemisorbed 2,4-DMQ. The spectra of 2,4-DMQ diluted in KBr, adsorbed on SiO_2 and on the BEA-1 zeolite, are presented in Figure 3, parts A and B. For spectra b and c, evacuation in a vacuum was carried out at 393 K and for spectrum d at 473 K. As with 2,6-DMQ, there are large similarities between spectra a and b. The silanol groups of SiO_2 interact with 2,4-DMQ molecules and evacuation at 473 K leads to a complete desorption. Furthermore, the spectra obtained for 2,4-DMQ adsorption on silica and on alumina are quite similar and, with alumina, there is also a complete disappearance of the 2,4-DMQ bands by vacuum treatment at 473 K. Therefore, the conclusions drawn for 2,6-DMQ adsorption on silica and alumina are also valid, i.e., 2,4-DMQ molecules can only be hydrogen bonded on silica (as could be expected from its weak acidity) but also on alumina: no strong interaction with Lewis sites due to steric constraints as previously proposed.[35]

This impossibility for 2,4-DMQ molecules to interact strongly with Lewis sites is confirmed by the similarities of the IR bands corresponding to 2,4-DMQ adsorbed on BEA-1 (very high concentration of Lewis sites) and BEA-2 (practically no Lewis sites) (Figure 2A,B, parts c and d). With both BEA samples, two new bands at 1646 (ν_{C-C}) and 3310 cm^{-1} (ν_{N-H}) are found in addition to the bands of hydrogen bonded 2,4-DMQ (Figure 3A,B, part b). The former band was previously observed in the spectra of 2,4-DMQ mixed with hydrochloric acid or adsorbed on silica alumina and on several large pore protonic zeolites.[35]

No change in the intensity of these bands occurs when the evacuation temperature is increased from 393 to 473 K whereas the band at 1570 cm^{-1} completely disappears and the intensity of the other bands corresponding to hydrogen bonded 2,4-DMQ on SiO_2 slightly decreases (see difference spectra in Figure 3A,B, part e). It can therefore be concluded that the spectra observed after desorption at 473 K correspond to 2,4-DMQ molecules chemically adsorbed on the protonic sites of BEA zeolites and hence to 2,4-dimethylquinolinium ions (2,4-DMQ^+). In agreement with this conclusion, the ratio between the intensities of the two characteristic bands found with the two

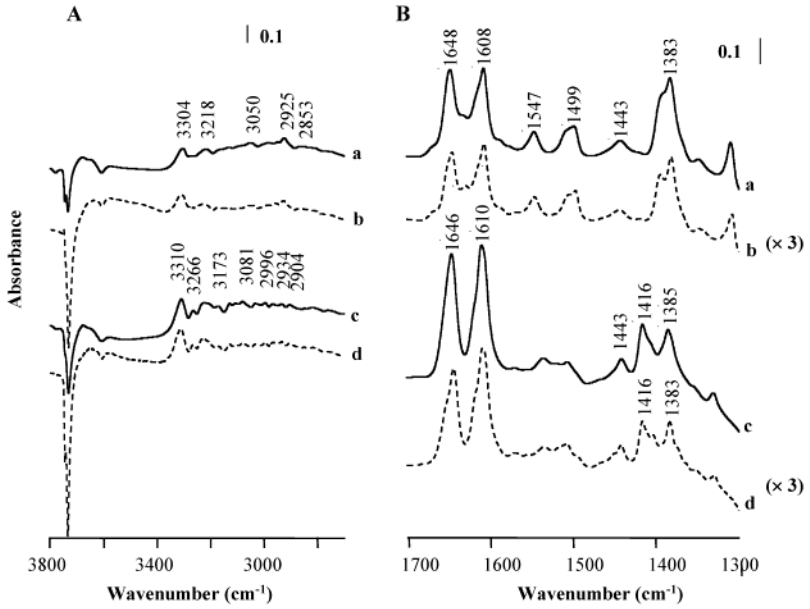

Figure 2. IR spectra of 2,6- (2,6-DMQ) (a, b) and 2,4-dimethylquinoline (2,4-DMQ) (c, d) adsorbed on BEA-1 (plain line) and -2 (dotted line) samples at 473 K (difference between the spectra after and before DMQ adsorption).

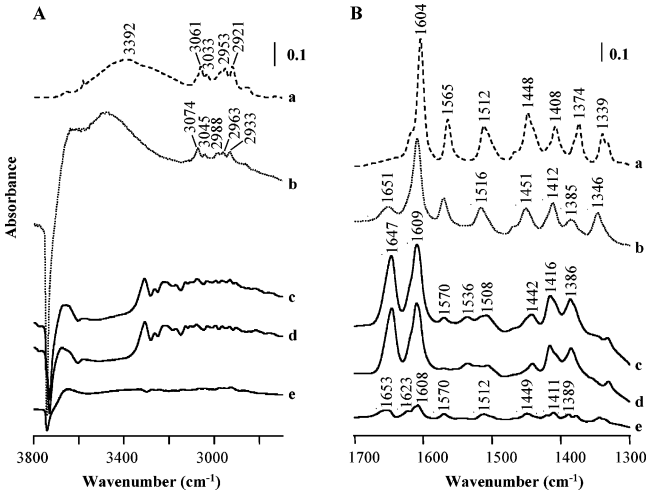

Figure 3. IR spectra of 2,4-dimethylquinoline (2,4-DMQ): (a) diluted in KBr; (b) adsorbed on SiO_2 at 393 K; (c, d) adsorbed on BEA-1 at 393 and 473 K, respectively (difference between the spectra after and before 2,4-DMQ adsorption); (e) difference spectrum (c − d).

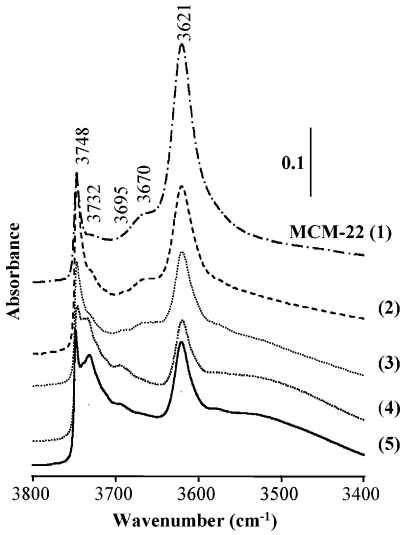

Figure 4. IR spectra of the hydroxyl region of the five activated H-MCM-22 samples.

BEA zeolites (BEA-1/BEA-2 = 2.9) is not very different from the ratio of their Brönsted sites concentrations (≈4.0) (Figure 2A,B, parts c and d).

3. Estimation of the Extinction Coefficients of 2,6- and 2,4-DMQ$^+$. The extinction coefficients were estimated for the bands at 1547 and 1649 cm^{-1} (2,6-DMQ$^+$) and at 1647 cm^{-1} (2,4-DMQ$^+$), from their intensity on BEA-1 and -2 samples and from the concentrations of Brönsted acid sites on these zeolites estimated by pyridine adsorption: 315 and 84 $\mu mol \cdot g^{-1}$ respectively.[32] It should be emphasized that there was an overlapping of the 1649 cm^{-1} band (2,6-DMQ$^+$) with other bands at 1656 and 1608 cm^{-1}, with as a consequence a lack of accuracy in the value of the extinction coefficient. It was not the case for the other bands. The values of the extinction coefficients ($cm \cdot \mu mol^{-1}$) are as follows. 2,6-DMQ$^+$: band at 1547 cm^{-1}, 0.5 ± 0.1; at 1649 cm^{-1}, 2.2 ± 0.6. 2,4-DMQ$^+$: at 1647 cm^{-1}, 3.3 ± 0.2.

4. Characterization of the H-MCM-22 Samples by Adsorption of Pyridine and 2,6- and 2,4-DMQ. 4.1. Hydroxyl Groups. The IR spectra of the activated H-MCM-22 samples are presented in Figure 4. All the spectra present a large and disymmetric band at 3621 cm^{-1} which corresponds to the three types of bridging hydroxyl groups: OH groups located in the supercages responsible for a band near 3620 cm^{-1}, located in the sinusoidal channels (band near 3605 cm^{-1}) and OH groups linked to the hexagonal prisms between two supercages (band near 3575 cm^{-1}).[36] As could be expected, the lower the Si/Al ratio of the zeolite (Table 1) the higher the intensity of the massif (MCM-22 (1) > (2) > (3) > (4) > (5)). A large massif can also be observed in the silanol region with a main peak at 3747 cm^{-1} due to isolated SiOH species on the external surface and large peaks at lower frequencies due either to silanols on the internal surface or to interacting silanols. In addition there is a small peak at 3695 cm^{-1} with samples MCM-22 (3), (4), and (5) and a larger one at 3670 cm^{-1} with samples MCM-22 (1), (2), and (3). These peaks are generally ascribed to AlOH species in which Al belong to extraframework aluminum species or are tricoordinated atoms linked to the framework.[4,11,37] Moreover, with MCM-22 (4) and (5), there is a broad adsorption band in

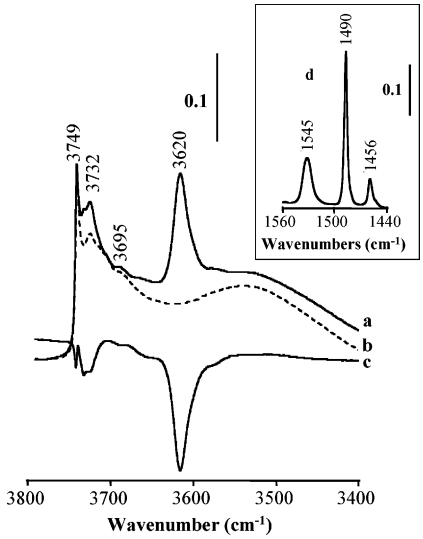

Figure 5. Effect of pyridine adsorption on the MCM-22 (5) sample at 423 K; (a) activated sample; (b) sample after pyridine adsorption and then desorption at 423 K; (c) difference spectrum (a − b); (d) IR spectrum of pyridine adsorbed at 423 K.

TABLE 2: Characterization of the H-MCM-22 Samples by Pyridine Adsorption Followed by IR Spectroscopy[a]

sample	Si/Al	acidity (μmol.g^{-1}) C_{Py+}	acidity (μmol.g^{-1}) C_{PyL}	I_{OH} (cm^{-1})	ϵ_{OH} (cm·μmol^{-1})
MCM-22 (1)	10	659	114	9.1	2.8
MCM-22 (2)	17	407	114	4.2	2.1
MCM-22 (3)	29	237	55	2.95	2.5
MCM-22 (4)	50	269	72	3.2	2.4
MCM-22 (5)	53	187	52	2.5	2.7

[a] C_{Py+}, C_{PyL}: concentrations of protonic and Lewis sites able to retain pyridine adsorbed at 423 K. I_{OH}: intensity ($\int A\, d\nu$) of the band at 3620 cm^{-1} for 10 mg of zeolite. ϵ_{OH}: extinction coefficient estimated for the band at 3620 cm^{-1}.

the 3700−3400 cm^{-1} region, which could correspond to hydrogen bonded silanol groups.[37]

4.2. Pyridine Adsorption. With all the H-MCM-22 samples, pyridine adsorption at 423 K resulted in the disappearance of the bands of bridging hydroxyl groups and in a slight decrease of the silanol massif as well as in the appearance of the bands corresponding to pyridinium ions (the most characteristic at 1545 cm^{-1}) and to pyridine bonded to Lewis sites (e.g., 1450 cm^{-1}) (Figure 5).

The concentrations of Brönsted and Lewis acid sites were calculated from the intensities of the bands at 1545 and 1450 cm^{-1} respectively, by using the values of the extinction coefficients: 1.13 and 1.28 cm·μmol^{-1} determined in a previous study.[26]

Table 2 shows that, like the intensity of the bridging OH band, the concentration of protonic sites able to retain pyridine adsorbed as pyridinium ions C_{Py^+} decreases as could be expected when the Si/Al ratio of the H-MCM-22 zeolite increases. A decrease in the concentrations of Lewis sites able to retain pyridine coordinated at 423 K (C_{PyL}) can also be observed. This can be related to an increase in hydrothermal stability with the Si/Al ratio of the zeolite and hence to a lower formation of extraframework Al species (EFAL) (which are Lewis acid sites), during the removal of the template by calcination. In agreement with this proposal, the intensity of the 3670 cm^{-1} band characteristic of hydroxylated EFAL species is much lower with the MCM-22 (3), (4), and (5) samples than with the MCM-22 (1) and (2) ones.

The intensity of the bridging OH groups I_{OH} obtained by difference between the spectra of the activated samples before and after pyridine adsorption at 423 K is roughly proportional to the concentration of the pyridinium ions at 420 K (C_{Py^+}). This suggests that most of the pyridinium ions result from protonation of pyridine on the bridging OH groups. If this supposition is admitted, an average extinction coefficient can be estimated from the formula: $\epsilon_{OH} = (I_{OH}\epsilon_{Py^+}/I_{Py^+})$ where I_{OH} and I_{Py^+} are the intensities of the bridging acidic OH band and of the pyridinium ions for the five H-MCM-22 samples and ϵ_{Py^+} the extinction coefficient of the pyridinium ion band at 1545 cm^{-1} (1.13 cm·μmol^{-1}). A value of 2.5 ± 0.3 cm·μmol^{-1} was obtained for ϵ_{OH} (Table 2).

4.3. 2,6-DMQ Adsorption. The adsorption of 2,6-DMQ was carried out on MCM-22 (4) and (5) only. With both samples, adsorption results in a decrease of the intensity of both silanol and bridging hydroxyl bands (Figure 6A). The significance of this decrease depends on the desorption temperature T_D as it is shown in Figure 6A for the MCM-22 (5) sample. With T_D = 393 K, a large part of silanol groups and half of the bridging OH groups interact with 2,6-DMQ molecules. Above 393 K, there is a significant decrease in 2,6-DMQ adsorption on silanol groups and an increase of the adsorption on the bridging OH groups. At 473 K, most of these latter interact with 2,6-DMQ, and all of them interact at 573 K. It should also be remarked that adsorption at 393 K leads to the formation of a large band between 3600 and 3400 cm^{-1} which disappears from 393 to 473 K (Figure 6A). This band is probably due to hydrogen bonding of 2,6-DMQ molecules with hydroxyl groups. Figure 6B shows the change in the intensity of the adsorbed 2,6-DMQ bands with T_D. The intensities of the two bands at 1549 and 1650 cm^{-1}, which are characteristic of the 2,6-dimethylquinolinium cations (2,6-DMQ$^+$), increase with T_D whereas the band at 1569 cm^{-1}, which is characteristic of hydrogen bonded 2,6-DMQ disappears at T_D = 473 K. This confirms the disappearance previously shown with BEA zeolites of the H-bonded 2,6-DMQ molecules from 473 K.

By using the extinction coefficients previously determined for the bridging OH band at 3620 cm^{-1} and for the 2,6-DMQ$^+$ bands at 1549 (a) and 1650 cm^{-1} (b), the concentrations of OH groups interacting with 2,6-DMQ (C_{OH}) and of 2,6-DMQ$^+$ ($C_{2,6-DMQ^+}$) were estimated. Whatever T_D, similar values of C_{OH} and $C_{2,6-DMQ^+}$ were obtained (Table 3). In agreement with Figure 6, there is an increase of C_{OH} and $C_{2,6-DMQ^+}$ when T_D increases from 393 to 473 K and even to 573 K. However, even at 573 K, these values are lower than those estimated by pyridine adsorption. This could be related to limitations in the diffusion of the bulky 2,6-DMQ molecules in the narrow intracrystalline pores of MCM-22 zeolite.

4.4. 2,4-DMQ Adsorption. With all the MCM-22 samples, 2,4-DMQ adsorption followed by desorption at T_D = 393 K results in a very low decrease of the bridging OH band, a significant decrease of the silanol bands as well as in the appearance of a large band between 3600 and 3400 cm^{-1} caused by hydrogen bonding of 2,4-DMQ molecules with hydroxyl groups. All that is shown in Figure 7A on the example of MCM-22 (5). The increase of T_D from 393 to 473 K causes a significant desorption of 2,4-DMQ from the silanol groups, a small desorption from the bridging OH groups as well as the disappearance of the large band between 3600 and 3400 cm^{-1}. When T_D is again increased (up to 673 K), there is practically no more change in the intensities of the band at 3620 cm^{-1} (bridging OH) and at 3747 cm^{-1} (external silanols) whereas the silanol bands at lower frequencies (internal silanols) are

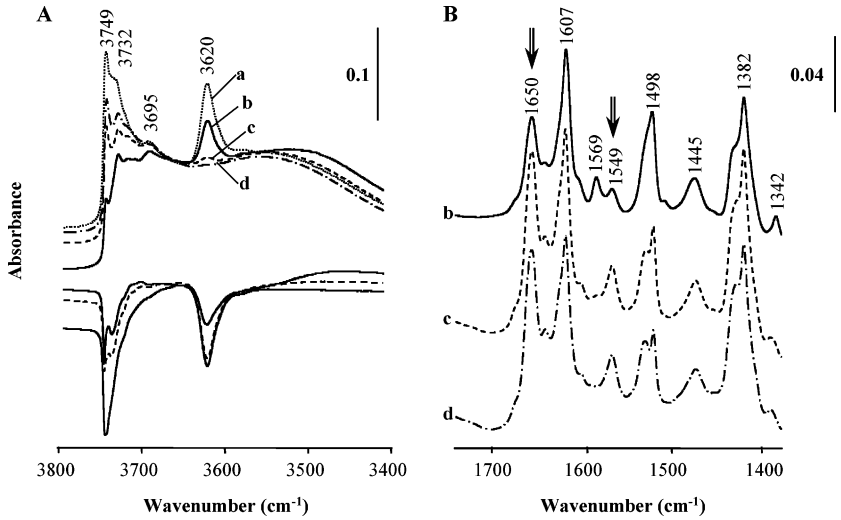

Figure 6. IR spectra of the hydroxyl region of the MCM-22 (5) sample after 2,6-DMQ adsorption (A) and of chemisorbed 2,6-DMQ (B): (a) activated sample, (b−d) desorption of 2,6-DMQ at 393, 473, and 573 K, respectively.

TABLE 3: Characterization of the H-MCM-22 Samples by 2,6-dimethylquinoline Adsorption Followed by IR Spectroscopy

sample	T_D[a] (K)	C_{OH} (μmol·g^{-1})	$C_{2,6-DMQ^+}$ (μmol·g^{-1})		C_{Py+} (μmol·g^{-1})
			a[b]	*b*[b]	
MCM-22 (4)	393	90	60	80	
	473	160	125	160	269[c]
	573	175	160	205	
MCM-22 (5)	393	105	55	80	
	473	170	110	170	186[c]
	573	180	120	165	

[a] T_D: desorption temperature. [b] *a*,*b*: determined from the intensities of the bands at 1547 and 1649 cm^{-1} respectively [c] T_D = 423 K

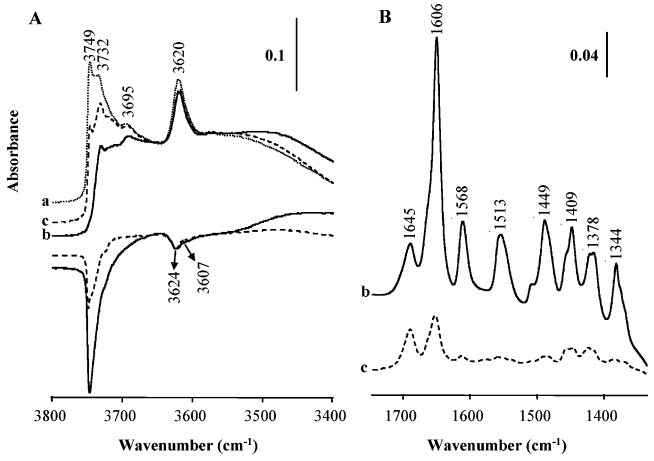

Figure 7. IR spectra of the hydroxyl region of the MCM-22 (5) sample after 2,4-DMQ adsorption (A) and of chemisorbed 2,4-DMQ (B): (a) activated sample; (b, c) desorption of 2,4-DMQ at 393 and 473 K, respectively.

completely recovered. In the difference spectra, the bridging OH groups interacting with 2,4-DMQ appear as two bands at 3624 and 3607 cm^{-1} (Figure 7A).

These frequency values correspond to those ascribed to bridging OH groups located in the supercages and the sinusoidal channels respectively.[36] The presence of these bands suggests that 2,4-DMQ molecules interact not only with the hydroxyl groups located in the outer pockets but also with part of those located in the intracrystalline pores. These inner bridging hydroxyl groups could be those located at the mouth of the pores

TABLE 4: Characterization of the H-MCM-22 Samples by 2,4-Dimethylquinoline Adsorption Followed by IR Spectroscopy

sample	T_D[a] (K)	C_{OH}	$C_{2,4-DMQ^+}$	$C_{2,4-DMQ^+} - C_{OH}$
MCM-22 (1)	393	60	115	55
	473	15	60	45
MCM-22 (2)	393	70	145	75
	473	55	95	40
	573	58	55	≈0
MCM-22 (3)	393	72	95	23
	473	40	65	25
	573	38	43	5
MCM-22 (4)	393	60	50	−10
	473	50	40	−10
MCM-22 (5)	393	40	50	10
	473	35	35	0

[a] T_D desorption temperature.

located on the surface of crystallites edges. However, the desorption of 2,4-DMQ from pore mouth sites should occur at low T_D values, which is not the case (T_D values > 673 K). Therefore, it has to be supposed that under the conditions of IR experiments, i.e., with a long contact time of 2,4-DMQ with the MCM-22 samples, a small part of 2,4-DMQ molecules enter the inner micropores. The penetration of these bulky molecules in the MCM-22 narrow pores is of course very difficult and hence is limited to the part of the inner pores close to the outer surface of crystallite edges.

There is a large change with T_D in the intensity of the bands corresponding to adsorbed 2,4-DMQ molecules. Thus, the increase of T_D from 393 to 473 K causes a significant decrease in the intensity of most of the bands except those at 1606 and 1645 cm^{-1} (Figure 7B). This indicates that for T_D = 393 K the interaction of most of the adsorbed 2,4-DMQ molecules with the zeolite was not very strong.

For all the H-MCM-22 samples, the concentrations of OH groups interacting with 2,4-DMQ (C_{OH}) and of 2,4-dimethylquinolinium ions ($C_{2,4-DMQ^+}$) were estimated by using the extinction coefficients previously determined for the bridging OH band and the 2,4-DMQ$^+$ band at 1645 cm^{-1}. With MCM-22 (1) and (2), $C_{2,4-DMQ^+}$ estimated for T_D = 393 and 473 K is much greater (2−4 times) than C_{OH}. It is slightly greater (1.3−1.6 times) with MCM-22 (3) whereas similar values are obtained with MCM-22 (4) and (5) samples (Table 4). Furthermore, the decrease of $C_{2,4-DMQ^+}$ caused by an increase of T_D is generally more significant than the decrease of C_{OH}: e.g., with MCM-22

TABLE 5: Catalytic Activity of the External Cups Acid Sites of Different H-MCM-22 Samples during *m*-Xylene Transformation at 350 °C for a Contact Time of 0.0087 h

sample	MCM-22 (1)	MCM-22 (2)	MCM-22 (3)	MCM-22 (4)
external surface area ($m^2 \cdot g^{-1}$)	49	114	102	59
conversion (%)[a]	3.0 (22%)	4.2 (48%)	2.6 (34%)	1.8 (27%)
selectivity				
p/*o*[b]	1.1 (3.8)	1.2 (2.2)	1.2 (2.1)	1.2 (2.6)
% isomerization[b]	98.0 (90.1)	98.1 (95.0)	98.4 (91.5)	98.3 (90.6)
Q (μmol.g^{-1})[c]	57 (9%)	69 (17%)	35 (15%)	27 (10%)
TOF (h^{-1})	572	667	804	741

[a] The values in parentheses correspond to the percentage of total conversion. [b] *p*/*o*: *p*- to *o*-xylene ratio. The values in parentheses were obtained on the fresh catalysts. [c] Quantity of 2,4-DMQ necessary to deactivate the external pockets. The values in parentheses correspond to the fraction of the total concentration of acid sites.

(2), $C_{2,4-DMQ^+}$ decreases of 50 and then of 40 μmol$\cdot g^{-1}$ are observed when T_D is increased from 393 to 473 and then 573 K, whereas only a decrease of 15 μmol$\cdot g^{-1}$ of C_{OH} can be observed when T_D passes from 393 to 473 K, C_{OH} remaining constant for T_D values between 473 and 573 K. Identical values of C_{OH} and $C_{2,4-DMQ^+}$ are observed for $T_D = 573$ K (Table 4). All that indicates that, at least for low T_D values, all the 2,4-dimethylquinolinium ions do not result from 2,4-DMQ adsorption on the bridging OH groups responsible for the bands at 3624 and 3607 cm^{-1} which were proposed above to be located in the inner pores.

The other acidic sites responsible for 2,4-DMQ protonation are most likely those located within the large outer cups. These sites would not retain 2,4-DMQ adsorbed above 573 K and hence would not be very strong.[38] It is difficult to ascribe one particular IR band to the corresponding hydroxyl groups. One possibility however could be the large band observed between 3730 and 3715 cm^{-1}, generally ascribed to internal silanols which interact with 2,4-DMQ at low temperatures and are completely rebuilt for $T_D > 623$ K. Another possibility could be the band at 3670 cm^{-1} assigned to hydroxyls linked to structural defects (i.e., still anchored to the zeolite framework) which are considered to be acidic.[38] One argument in favor of this proposal is that this band is only clearly apparent for MCM-22 (1), (2), and (3), for which $C_{2,4-DMQ^+}$ is much greater than C_{OH} (Table 4). Last, it could not be excluded that the weakly acidic hydroxyl groups are not visible in the IR spectra because of interaction with neighboring species such as silanol groups, which could be the case for bridging OH groups located in the external pockets.

The concentration of these outer pockets acid sites could be estimated by the difference between $C_{2,4-DMQ^+}$ and C_{OH} at the lower T_D value (393 K). For four of the samples, the difference is positive, but for MCM-22 (4) a negative value is obtained (Table 4). This negative value could result from the large imprecision in the determination of C_{OH}. Indeed, the same extinction coefficient was used for the two hydroxyl bands observed at 3624 and 3607 cm^{-1}.

This concentration of outer pocket sites is very low compared to the total concentration of protonic sites measured by pyridine adsorption: 8.5, 18.5, 10.5, and 5.5%, respectively, of this concentration for MCM-22 (1), (2), (3), and (5) respectively (Table 4). Furthermore, as could be expected, the percentages are quite proportional to the external surface area of the samples: 49, 114, 110, and 33 $m^2 \cdot g^{-1}$ respectively.

5. Estimation of the Concentration of the External Sites Active in *m*-Xylene Transformation. The procedure previously developed in order to estimate the concentration of the external active sites and their activity and selectivity[19] was applied to the H-MCM-22 samples. The effect of time-on-stream (TOS) was compared for the transformation of *m*-xylene pure or added with 2,4-DMQ. In both cases, there is an initial decrease in conversion followed by a quasi plateau for TOS >20−40 min. The decrease is more significant in the presence of 2,4-DMQ. The difference between *m*-xylene conversion in absence and in the presence of 2,4-DMQ (ΔX) corresponds to the poisoning effect of 2,4-DMQ (Figure 8). As previously shown, under the operating conditions, 2,4-DMQ poisons the external acid sites only, without blocking the access to the inner sites.

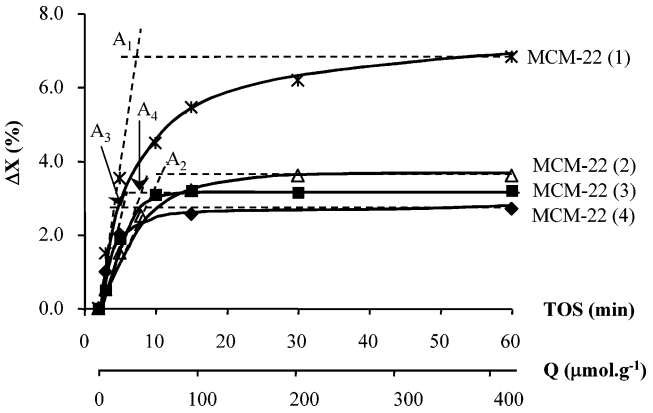

Figure 8. Decrease in *m*-xylene conversion (ΔX) due to 2,4-DMQ poisoning as a function of time-on-stream (TOS) for the MCM-22 (1), (2), (3), and (4) samples.

Therefore, the maximum ΔX value corresponds to the conversion of *m*-xylene on the external sites. Table 5 shows that this latter conversion corresponds to 22, 48, 35, and 27% of the total conversion on the MCM-22 (1), (2), (3), and (4) samples, respectively, for example, is quite proportional to the outer surface area of the samples. This is in agreement with a selective poisoning of the outer acidic sites.

The distribution of the products formed on the external sites can be deduced from the difference between the yields obtained after the initial deactivation in absence and in the presence of 2,4-DMQ.[19] With the four samples (Table 5), isomerization is practically the only reaction (> 98%), the other products resulting from disproportionation. The *p*- to *o*-xylene ratio (*p*/*o*) is the one expected from a non shape selective isomerization (1.1−1.2), in agreement with the large size of the external pockets. This selectivity is a strong argument in favor of a selective poisoning of the outer acid sites by 2,4-DMQ molecules.

Furthermore, if it is admitted that at short TOS values, all the DMQ molecules passing on the zeolite have a poisoning effect, the values of TOS and of the amount of 2,4-DMQ necessary to obtain the maximum deactivation (*Q*) will be given by points A_1, A_2, A_3 and A_4 for samples MCM-22 (1), (2), (3), and (4) respectively (Figure 8). Whatever the sample, the *Q* values are much lower than the concentration of protonic sites (C_{Py^+}) able to retain pyridine adsorbed at 423 K: 9, 17, 15,

and 10% of this concentration for MCM-22 (1), (2), (3), and (4), respectively (Table 5). The first three values are very close to those estimated by 2,4-DMQ adsorption: $(C_{2,4-DMQ^+})_{393K} - C_{OH}$. In addition, there is a quasiproportionality between the four values and the external surface areas of the H-MCM-22 samples, which is in agreement with a selective poisoning of the outer acid sites.

For the four samples, the concentration of active outer sites is lower than that of 2,4-dimethylquinolinium ions ($C_{2,4-DMQ^+}$) estimated for $T_D = 393$ or 473 K (Table 4). This confirms that part of the sites which are able to protonate 2,4-DMQ are not located in the outer pockets.

Turnover frequency values of the outer acid sites estimated from the activity and *Q* values are very close for the four H-MCM-22 samples: 570, 670, 800, and 740 h^{-1} (Table 5). These values are slightly lower than those found for *m*-xylene transformation over FAU zeolites (850−1050 h^{-1})[39] but higher than those on silica alumina (100 h^{-1}).[40] This suggests that the outer pocket acid sites have catalytic properties similar to those of zeolites.

Conclusion

The following conclusions can be drawn from the IR study of 2,6- and 2,4-dimethylquinoline adsorption over H-MCM-22 zeolites.

1. The comparison of the spectra of dimethylquinoline (DMQ) pure or adsorbed on silica, alumina and BEA zeolites shows that (i) all the physisorbed and hydrogen bonded species can be eliminated by evacuation above 473 K, (ii) there exist some characteristic bands corresponding to dimethylquinolinium ions which can be used for a quantitative estimation of these species, and (iii) because of steric hindrance, DMQ molecules do not interact with Lewis sites.

2. As could be expected from poisoning experiments, 2,6-DMQ can be protonated at temperatures higher than 473 K on most of the acid sites able to protonate pyridine.

3. The bulkier 2,4-DMQ molecules interact with protonic sites of inner micropores (IR bands at ≈ 3620 cm^{-1}) located near the outer surface of crystallite edges. This penetration within the inner pores, which does not occur during poisoning experiments, can be related to the long contact time of 2,4-DMQ molecules with the zeolite sample during IR experiments. Protonation of 2,4-DMQ occurs also on the bridging hydroxyl groups located in the external pockets; these hydroxyl groups do not vibrate at 3620 cm^{-1}. Their concentration can be roughly estimated by the difference between the concentrations of 2,4-dimethylquinolinium ions $C_{2,4-DMQ^+}$ and of bridging hydroxyl groups C_{OH} (IR bands at ≈ 3620 cm^{-1}) which interact with 2,4-DMQ molecules at 393 K.

4. In agreement with the above proposal, the concentration of external acid sites active in *m*-xylene transformation at 623 K (determined through poisoning experiments with 2,4-DMQ) was found to be close to this difference. Therefore, 2,4-DMQ adsorption can be applied for estimating the concentration of the external pocket protonic sites. The validity of this method was confirmed with MCM-36 samples.[41] With these samples, the concentration of acidic bridging OH groups responsible for the large band at 3620 cm^{-1} is very small in comparison to that of 2,4-dimethylquinolinium ions. Again, a good agreement was found between the concentration of active external sites and the $((C_{2,4-DMQ^+})_{393K} - C_{OH})$ difference.

5. As could be expected, the percentages of acidic sites located within the external pockets and of external active sites are proportional to the external surface areas of the H-MCM-22 samples. This indicates that 2,4-DMQ chemisorption followed by IR spectroscopy is a suitable method for characterizing the outer acidity of MCM-22 zeolite.

6. The turnover frequencies (TOF) of the outer active sites of H-MCM-22 are slightly lower than the one of non shape selective zeolites such as FAU but several times greater than the TOF of the protonic sites of amorphous silica−alumina. Therefore, the protonic sites located in the outer pockets seem to be similar in behavior with the protonic sites of large pore zeolites.

Acknowledgment. S.L. acknowledges warmly Prof. A. Corma and V. Fornes for welcoming him for 3 months in the Instituto de Tecnologia Quimica of Valencia (Spain) in order to synthesize the MCM-22 zeolite samples used in this work.

References and Notes

(1) Rubin, M. K.; Chen, P. U.S. Patent 4,954,325, 1990 (assigned to Mobil Oil Corporation).
(2) Leonowicz, M. E.; Lawton, S. L.; Partridge, R. D.; Chu, P.; Rubin, M. K. *Science* **1994**, *264*, 1910.
(3) Lawton, S. L.; Leonowicz, M. E.; Partridge, R. D.; Chu, P.; Rubin, M. K. *Microporous Mesoporous Mater.* **1998**, *23*, 109.
(4) Corma, A.; Corell, C.; Perez-Pariente, J. *Zeolites* **1995**, *15*, 2.
(5) Millini, R.; Perego, G.; Parker Jr, W. O.; Bellussi, G.; Carluccio, L. *Micropor. Mater.* **1995**, *4*, 221.
(6) Corma,A.; Corell, C.; Martinez, A.; Perez-Pariente, J. *Stud. Surf. Sci. Catal.* **1994**, *84*, 859.
(7) Corma,A.; Corell, C.; Llopis, F.; Martinez, A.; Perez-Pariente, J. *Appl. Catal. A: Gen.* **1994**, *115*, 121.
(8) Corma,A.; Martinez, A.; Martinez, C. *Catal. Lett.* **1994**, *28*, 187.
(9) Corma,A.; Gonzàlez-Alfaro, V.; Orchillès, A. V. *Appl. Catal., A: Gen.* **1995**, *129*, 203.
(10) Corma, A.; Martinez-Triguero, J. *J. Catal.* **1997**, *165*, 102.
(11) Unverricht, S.; Hunger, M.; Ernst, S.; Karge, H. G.; Weitkamp, J. *Stud. Surf. Sci. Catal.* **1994**, *84*, 37.
(12) Karge, H. G.; Ernst, S.; Weihe, M.; Weiβ, U.; Weitkamp, J. *Stud. Surf. Sci. Catal.* **1994**, *84*, 1805.
(13) Souverijns, W.; Verrelst, W.; Vanbutsele, G.; Martens, J. A.; Jacobs, P. A. *J. Chem. Soc., Chem. Commun.* **1994**, 1671.
(14) Meriaudeau, P.; Tuan, Vu A.; Nghiem, Vu T.; Lefebvre, F.; Ha, Vu T. *J. Catal.* **1999**, *185*, 378.
(15) Park, S.-H.; Rhee, H.-K. *Catal. Today* **2000**, *63*, 267.
(16) Corma, A.; Martinez-Soria, V.; Schnoeveld, E. *J. Catal.* **2000**, *192*, 163.
(17) Beck, J. S.; Dandekar, A. B.; Degnan, T. F. *Zeolites for Cleaner Technologies*, Catalytic Science Series Vol. 3; Imperial College Press: London, 2002; p 223.
(18) Du, H.; Olson, D. H. *J. Phys. Chem. B* **2002**, *106*, 395.
(19) Laforge, S.; Martin, D.; Guisnet, M. *Microporous Mesoporous Mater.* **2004**, *67*, 235.
(20) Corma, A.; Fornes, V.; Forni, L.; Marquez, F.; Martinez-Triguero, J.; and Moscotti, D. *J. Catal.* **1998**, *179*, 451.
(21) Wang, Y.; Zhuang, J.; Yang, G.; Zhou, D.; Ma, D.; Han, X.; Bao, X. *J. Phys. Chem. B* **2004**, *108*, 1386.
(22) Meriaudeau, P.; Tuel, A.; Vu, T. T. H. *Catal. Lett.* **1999**, *61*, 89.
(23) Laforge, S.; Martin, D.; Paillaud, J. L.; Guisnet, M. *J. Catal.* **2003**, *220*, 92.
(24) Leofanti, G.; Padovan, M.; Tozzola, G.; Venturelli, B. *Catal. Today* **1998**, *41*, 207.
(25) He, Y. J.; Nivarthy, G. S.; Eder, F.; Seshan, K.; Lercher, J. A. *Microporous Mesoporous Mater.* **1998**, *25*, 207.
(26) Guisnet, M.; Ayrault, P.; Datka, J. *Pol. J. Chem.* **1997**, *71*, 1455.
(27) Ravishankar, R.; Bhattacharya, D.; Jacob, N. E.; Sivasanker, S. *Micropor. Mater.* **1995**, *4*, 83.
(28) Kumar, N.; Lindfors, L.-E. *Appl. Catal., A: General* **1996**, *147*, 175.
(29) Corma, A. *Microporous Mesoporous Mater.* **1998**, *21*, 487.
(30) Wu, P.; Komatsu, T.; Yashima, T. *Microporous Mesoporous Mater.* **1998**, *22*, 343.
(31) Meloni, D.; Laforge, S.; Martin, D.; Guisnet, M.; Rombi, E.; Solinas, V.; *Appl. Catal., A: Gen.* **2001**, *215*, 55.
(32) Marques, J. P.; Gener, I.; Ayrault, P.; Bordado, J. C.; Lopes, J. M.; Ramôa Ribeiro, F.; Guisnet, M. *Microporous Mesoporous Mater.* **2003**, *60*, 251.
(33) Benesi, H. A. *J. Catal.* **1973**, *28*, 176.

(34) Jacobs, P. A.; Heylen, C. F. *J. Catal.* **1974**, *34*, 267.
(35) Kim, J.-H.; Ishida, A.; Miki, N. React. Kinet. *Catal. Lett.* **1999**, *67* (2), 281.
(36) Onida, B.; Geobaldo, F.; Testa, F.; Crea, F.; Garrone, E. *Microporous Mesoporous Mater.* **1999**, *30*, 119.
(37) Corma,A.; Corell, C.; Fornes, V.; Kolodziejski, W.; Perez-Pariente, J. *Zeolites* **1995**, *15*, 576.
(38) Onida, B.; Borello, L.; Borelli, B.; Geobaldo, F.; Garrone, E. *J. Catal.* **2003**, *214*, 191.
(39) Morin, S.; Ayrault, P.; Gnep, N. S.; Guisnet, M. *Appl. Catal., A: Gen.* **1998**, *166*, 281.
(40) Morin, S.; Ayrault, P.; El Mouahid, S.; Gnep, N. S.; Guisnet, M. *Appl. Catal., A: Gen.* **1997**, *159*, 317.
(41) Laforge, S. Unpublished results.